Paper

Blind frequency offset estimation for overlap PCC-OFDM systems in presence of phase noise

Jinwen Shentu and Jean Armstrong

Abstract — This paper presents a technique for frequency offset estimation for polynomial cancellation coded orthogonal frequency division multiplexing with symbols overlapped in the time domain (overlap PCC-OFDM) in the presence of phase noise. The frequency offset estimator is designed based on the subcarrier pair imbalance (SPI) caused by frequency offset. The estimation is performed in the frequency domain at the output of the receiver discrete Fourier transform (DFT). No training symbols or pilot tones are required. Simulations show that this estimator is an approximately linear function of frequency offset. Phase noise does not significantly affect the variance performance of the estimator.

Keywords — OFDM, frequency offset, estimation, phase noise, overlap PCC-OFDM.

1. Introduction

Orthogonal frequency division multiplexing (OFDM) techniques have been widely used as the modulation method in many high-speed data transmission systems [1, 2]. One of the major disadvantages is its high sensitivity to frequency offset caused by the frequency difference between the oscillators in the transmitter and the receiver. A frequency offset will introduce a common phase error (CPE) in all subcarriers in a symbol, will cause noise-like intercarrier interference (ICI) crossing all subcarriers in a symbol and reduce the amplitude of the wanted signal. Since phase noise will cause CPE and ICI, OFDM is also very sensitive to phase noise [3].

Polynomial cancellation coded OFDM is an ICI cancellation scheme which was originally designed to reduce the ICI caused by frequency offset rather than phase noise [4–6]. A recent study shows that PCC-OFDM can also significantly reduce the ICI caused by phase noise [7]. Furthermore, it is shown in [8] that in PCC-OFDM systems where the symbols are entirely coded in PCC, blind frequency offset estimation can be achieved by exploiting the subcarrier pair imbalance caused by frequency offset.

In PCC-OFDM, each data value to be transmitted is mapped onto a group of subcarriers. The number of subcarriers in a group depends on the requirement for the system performance [6]. In this paper, the case where each data value to be transmitted is mapped onto a pair of subcarriers is considered. PCC-OFDM has many advantages including insensitivity to frequency offset and Doppler spread, much faster power spectrum roll-off and much lower out-of-band power than conventional OFDM. Despite its advantages, PCC-OFDM is not bandwidth efficient in its simplest form. One way to overcome this drawback is to overlap PCC-OFDM symbols in the time domain [9, 10]. Figure 1 shows how PCC-OFDM symbols are overlapped with an overlapping offset of $T/2$, where T is the symbol period. In this case, the first half of the current PCC-OFDM symbol is overlapped with the second half of the previous PCC-OFDM symbol. The second half of the current symbol is overlapped with the first half of the next PCC-OFDM symbol. Using the overlapping technique, the same data rate as conventional OFDM can be achieved while the benefits of PCC-OFDM are retained. After the overlapping, at any time instant an overlap PCC-OFDM symbol contains overlapping components from adjacent PCC-OFDM symbols. In this paper we propose a frequency offset estimator for overlap PCC-OFDM, which has the same form of the estimator as that we proposed for PCC-OFDM [8].

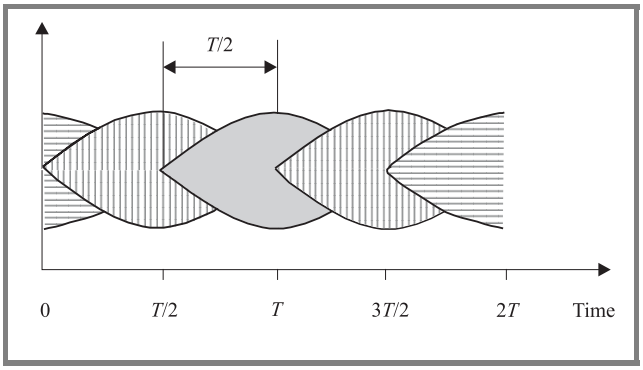

Fig. 1. PCC-OFDM symbols overlapped in the time domain.

This paper is organized as follows. Sections 2 and 3 are the background for overlap PCC-OFDM techniques. They are essential for understanding the frequency offset estimation in overlap PCC-OFDM. In Section 2, the basic concepts for overlap PCC-OFDM are introduced and an overlap OFDM system is described. In Sections 3 and 4, the SPI which is the basis of the technique of frequency offset estimation is investigated, and the expression for a demodulated overlap PCC-OFDM subcarrier is derived. In Section 5, the frequency offset estimator for overlap PCC-OFDM is

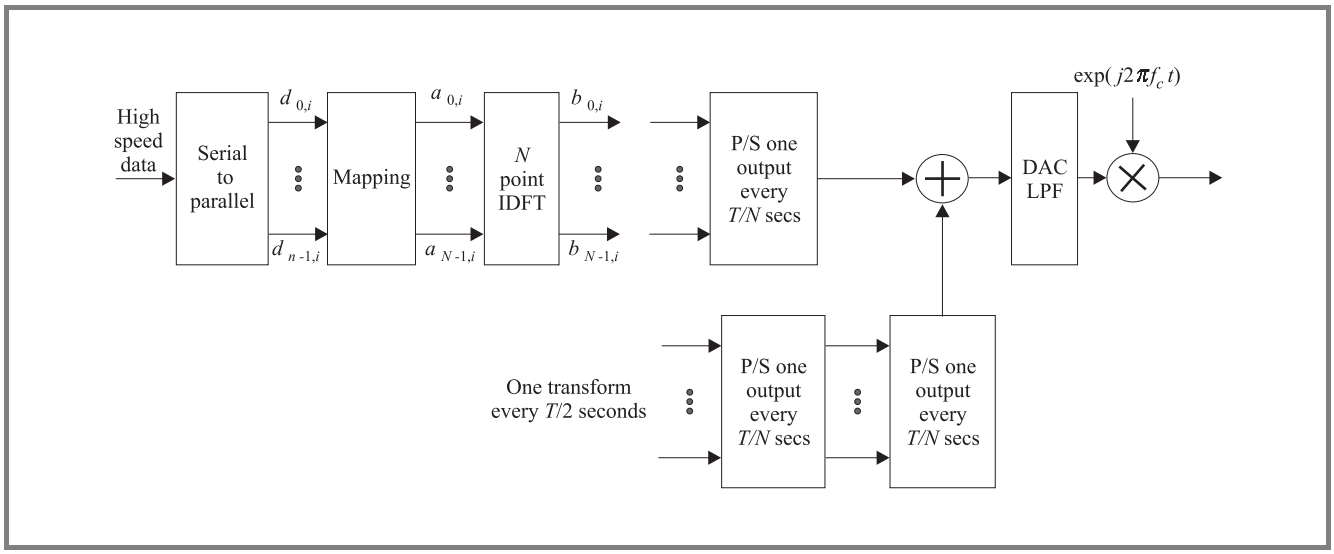

Fig. 2. Transmitter for an overlap PCC-OFDM system.

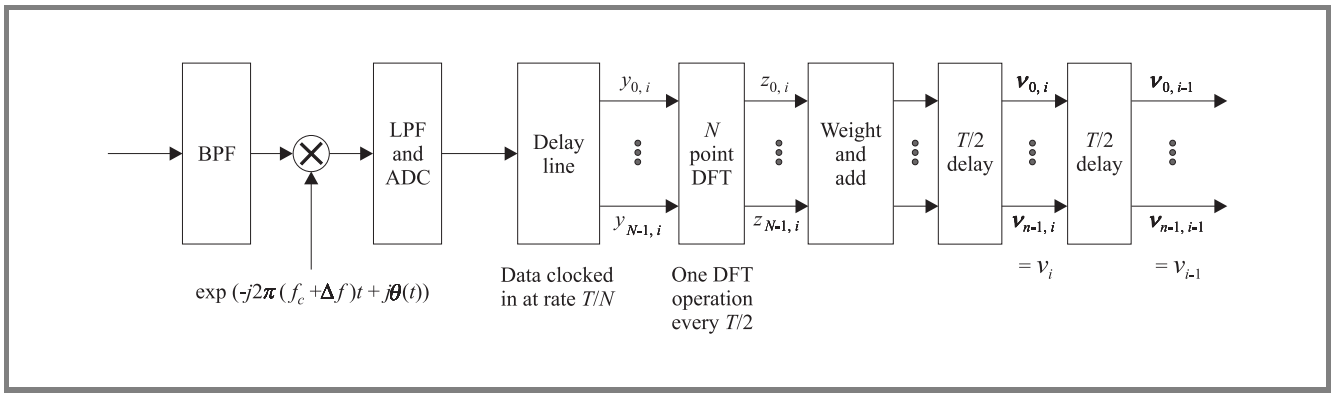

Fig. 3. Receiver for an overlap PCC-OFDM system.

introduced. In Sections 6 and 7, the effects of phase noise on the performance of the PCC-OFDM and the estimator have been evaluated. In Section 8, numerical simulation results are presented and the performance of the estimator is evaluated. Conclusions are drawn in Section 9.

2. An overlap PCC-OFDM system

We will now look into an overlap PCC-OFDM system. For the convenience of description, we define a symbol before overlapping as a PCC-OFDM symbol and define a symbol containing overlapping components as an overlap PCC-OFDM symbol.

Figure 2 shows the block diagram of an overlap PCC-OFDM transmitter. $d_{0,i}, \ldots, d_{n-1,i}$ are n data values in the ith data block to be transmitted. They are mapped onto N subcarriers $a_{0,i}, \ldots, a_{N-1,i}$, where N is a power of 2. In the case of data being mapped onto pairs of subcarriers, we have $n = N/2$ and $a_{2M+1,i} = -a_{2M,i}$. The output vectors of the inverse discrete Fourier transform (IDFT) are then overlapped in the way described in Fig. 1. After the parallel to serial conversion (P/S), the digital to analog conversion (DAC) and low pass filtering (LPF), the overlap PCC-OFDM symbol is up converted into the radio frequency (RF) signal.

Figure 3 shows the block diagram of an overlap PCC-OFDM receiver. The received signal is fed into a band pass filter (BPF) and down converted into a baseband signal. The frequency offset Δf is introduced. For convenience, the normalized frequency offset ΔfT is represented by ε. After the LPF and analog to digital conversion (ADC), a sequence of samples of the baseband signal is obtained. The data samples are clocked into the delay line at rate T/N and converted into parallel data blocks, each block has N data values. One DFT operation is performed on each block for every $T/2$ second.

The output of the DFT is then weighted and added to obtain the estimates of the transmitted data. The technique for

data recovery from a set of overlapped symbols has been presented in the reference [9]. A two-dimensional minimum mean square error (MMSE) equalizer can effectively recover the overlapped symbols. The equalization of the overlap PCC-OFDM systems is beyond the range of this paper, more detailed discussions can be found in the reference [9].

3. Subcarrier pair imbalance in PCC-OFDM in absence of phase noise

In overlap PCC-OFDM, each demodulated subcarrier contains overlapping components from adjacent PCC-OFDM symbols [11]. The SPI is defined as the amplitude or power difference between two subcarriers in a demodulated subcarrier pair. That is

$$F(\Delta fT) = \left|z_{2M+1,i}\right|^2 - \left|z_{2M,i}\right|^2. \tag{1}$$

Each value of imbalance is a combination of the imbalance of the PCC-OFDM subcarrier pair and the imbalance of the overlapping components in the demodulated subcarrier pair.

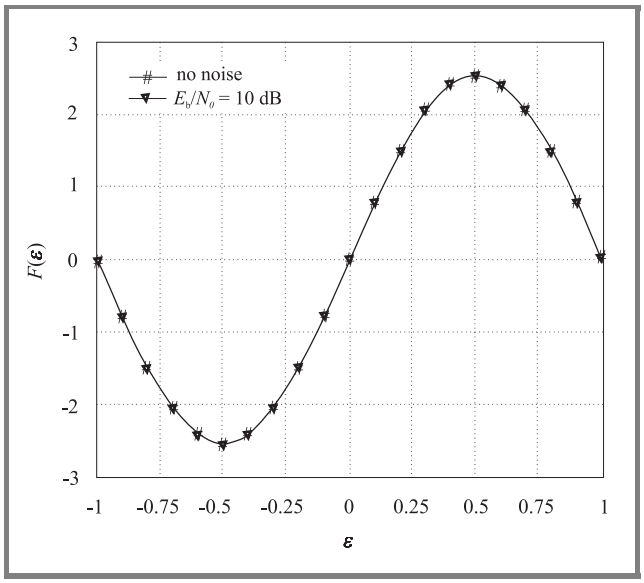

Fig. 4. Average SPI as a function of frequency offset for $N = 128$, 300 symbols.

In the absence of frequency offset, two demodulated subcarriers in an overlap PCC-OFDM subcarrier pair are balanced in a particular way. The SPI depends not only on the frequency offset and transmitted data values in the current PCC-OFDM symbol, but also on the overlapping components from the preceding and following PCC-OFDM symbols. The data dependency in overlap PCC-OFDM can be removed by averaging over a number of subcarrier pairs. The average SPI depends on the frequency offset, therefore, we can use the average imbalance for frequency offset estimation.

Figure 4 shows the average SPI as a function of frequency offset for $N = 128$. The number of simulated symbols was 300 and all subcarrier pairs were used. The figure shows some interesting features:

- Crossing zero at zero frequency offset.
- For $|\varepsilon| < 0.5$, the SPI increases monotonically as the frequency offset increases.
- Additive white Gaussian noise (AWGN) does not affect the zero crossing position.
- The frequency estimation range can be extended to one subcarrier spacing.

4. Expression for an overlap PCC-OFDM subcarrier

To investigate the relationship between the SPI and the frequency offset more clearly, the expression of an OFDM signal must be derived. The *k*th sample in the *i*th time domain symbol in PCC-OFDM is given by [12]

$$b_{k,i} = \frac{1}{N}\sum_{l=0}^{N-1} a_{l,i} \exp\left(\frac{j2\pi kl}{N}\right), \tag{2}$$

where $a_{l,i}$ is the signal in the *l*th subcarrier in the *i*th OFDM symbol. The overlapping components in the current symbol are introduced from the second half of the $(i-1)$th PCC-OFDM symbol and the first half of the $(i+1)$th PCC-OFDM symbol. The *k*th overlapping component is given by [11]

$$b'_{k,i} = \begin{cases} \dfrac{1}{N}\displaystyle\sum_{l=0}^{N-1}(-1)^l a_{l,i-1}\exp\left(\frac{j2\pi kl}{N}\right), & \text{for } 0 \le k \le N/2-1, \\ \dfrac{1}{N}\displaystyle\sum_{l=0}^{N-1}(-1)^l a_{l,i+1}\exp\left(\frac{j2\pi kl}{N}\right), & \text{for } N/2 \le k \le N-1. \end{cases} \tag{3}$$

At the receiver, the *k*th value of the *i*th input data block to the DFT is given by

$$y_{k,i} = \exp\left(\frac{j2\pi k\varepsilon}{N}\right)\left(b'_{k,i} + b_{k,i}\right) + w_{k,i}, \tag{4}$$

where $w_{k,i}$ is the channel AWGN. The mth subcarrier in the ith demodulated symbol is then given by

$$z_{m,i} = \sum_{k=0}^{N-1} y_{k,i} \exp\left(\frac{-j2\pi km}{N}\right) =$$

$$= \sum_{k=0}^{N/2-1} y_{k,i} \exp\left(\frac{-j2\pi km}{N}\right) + \sum_{k=N/2}^{N-1} y_{k,i} \exp\left(\frac{-j2\pi km}{N}\right). \quad (5)$$

The $2M$th demodulated subcarrier is given by

$$z_{2M,i} = \sum_{L=0}^{N/2-1} (CF_{2(L-M)} + CF_{2(L-M)+1}) d_{L,i-1} + \\ + \sum_{L=0}^{N-1} (CS_{2(L-M)} + CS_{2(L-M)+1}) d_{L,i+1} + \\ + \sum_{L=0}^{N-1} (c_{2(L-M)} - c_{2(L-M)+1}) d_{L,i} + W_{2M,i}, \quad (6)$$

where $W_{2M,i}$ is the DFT of $w_{k,i}$, c_{l-m} are complex coefficients given by [4]

$$c_{l-m} = \frac{\sin\big(\pi(l-m+\varepsilon)\big)}{N \sin\big(\pi(l-m+\varepsilon)/N\big)} \times \exp\big(j\pi(N-1)(l-m+\varepsilon)/N\big). \quad (7)$$

It is shown in [13], $W_{2M,i}$ is AWGN. The coefficients CF_{l-m} and CS_{l-m} are given by

$$CF_{l-m} = \frac{1}{N} \sum_{k=0}^{N/2-1} \exp\left(\frac{j2\pi k(l-m+\varepsilon)}{N}\right), \quad (8)$$

$$CS_{l-m} = \frac{1}{N} \sum_{k=N/2}^{N-1} \exp\left(\frac{j2\pi k(l-m+\varepsilon)}{N}\right). \quad (9)$$

Similarly, the $(2M+1)$th demodulated subcarrier can be obtained.

5. Minimum mean square error frequency offset estimator for overlap PCC-OFDM

It is shown in Appendix A that Eq. (1) for overlap PCC-OFDM for 4 quadrature amplitude modulation (4QAM) can be written as

$$F(\varepsilon) = K \sin(\pi\varepsilon) + e_M, \quad (10)$$

where K is a constant given by [8]

$$K = \cos\left(\frac{\pi}{N}\right) \prod_{k=1}^{\log_2(N)-1} \cos\left(\frac{2^{k-1}\pi}{N}\right) \quad (11)$$

e_M is the error term. For small frequency offset, the error term can be approximated as additive noise with zero mean and finite variance. Applying MMSE techniques for Eq. (10) [14], we can obtain the frequency offset estimator

$$\hat{\varepsilon} = \frac{1}{\pi} \sin^{-1}\left(\frac{1}{KM_l} \sum_{t=1}^{M_l} F_t(\varepsilon)\right), \quad (12)$$

where M_l is number of subcarrier pairs used for the frequency offset estimation.

6. Phase noise in PCC-OFDM

The effects of phase noise on the performance of PCC-OFDM have been investigated in [15]. For convenience of discussion, the main results are outlined as follows. Let

$$\psi_p = \frac{1}{N} \sum_{k=0}^{N-1} \exp\left(\frac{-j2\pi kp}{N}\right) \exp\big(j\theta(k)\big), \quad (13)$$

where $p = -(N-1), \ldots, 0, \ldots, (N-1)$, $\theta(k)$ is the kth sample of the phase noise. Thus the quantity ψ_p is the DFT of $\exp\big(j\theta(k)\big)$, evaluated at the frequency p/N. Variable ψ_p depends on the frequency spectrum of the phase noise. If $\theta(k)$ is a constant, then $\psi_p = 0$, for $p \neq 0$, and there is no ICI. Furthermore, for $\theta(k) = 0$, we obtain $\psi_p = 1$, and the demodulated subcarrier is equal to its original data to be transmitted. For a small phase noise $\theta(k)$, using the approximation $\exp\big(j\theta(k)\big) \approx 1 + j\theta(k)$, Eq. (13) can be written as

$$\psi_p \approx \frac{1}{N} \sum_{k=0}^{N-1} \exp\left(\frac{-j2\pi kp}{N}\right) \big(1 + j\theta(k)\big). \quad (14)$$

For $p \neq 0$, Eq. (14) is given by

$$\psi_p \approx \frac{j}{N} \sum_{k=0}^{N-1} \exp\left(\frac{-j2\pi kp}{N}\right) \theta(k). \quad (15)$$

Quantity ψ_p is presented in terms of the DFT of the phase noise, which is the spectrum of the phase noise $\theta(k)$. For $p = 0$, we get

$$\psi_p \approx 1 + \frac{j}{N} \sum_{k=0}^{N-1} \theta(k). \quad (16)$$

The estimate of the Mth data value in the ith data block to be transmitted is given by

$$v_{M,i} = d_{M,i} + \frac{1}{2} d_{M,i} \big[-\psi_{-1} + 2(\psi_0 - 1) - \psi_1 \big] + \\ + \frac{1}{2} \sum_{\substack{L=0 \\ L \neq M}}^{N/2-1} d_{L,i} \big(-\psi_{2(M-L)+1} + 2\psi_{2(M-L)} - \psi_{2(M-L)-1} \big) \\ + \big(W_{2M,i} - W_{2M+1,i}\big)/2, \quad (17)$$

where the first term at the right hand is the wanted signal, the second term is the CPE, the third term is the ICI and the last one is the weighted AWGN. In OFDM, the CPE and ICI depend on the individual frequency spectrum of the phase noise [3, 16]. In PCC-OFDM, the CPE and ICI depend on the combinations of phase noise spectra rather than individual spectra. This makes it possible to reduce the effects of phase noise by using a phase lock loop (PLL) that can fit the overall phase noise spectrum to a particular pattern. For the special case where the individual spectrum ψ_p has a linear relationship with frequency, then the ICI caused by the phase noise can be completely cancelled.

The CPE term is given by

$$Y_{CM,i} = \frac{1}{2} d_{M,i}\left[-\psi_{-1} + 2(\psi_0 - 1) - \psi_1\right] = j d_{M,i}\Theta_0 \quad (18)$$

where Θ_0 is a constant,

$$\Theta_0 = \frac{2}{N}\sum_{k=0}^{N-1} \sin^2\left(\frac{\pi k}{N}\right)\theta(k). \quad (19)$$

This result indicates that all PCC-OFDM subcarriers experience a CPE. This rotation can be detected and therefore compensated using techniques provided in the literature [17]. One simple way to do this is to insert pilot tones in a symbol and estimate the rotation angle. Once the CPE is corrected in the pilot tones, the remaining phase noise in other subcarriers can be corrected.

Similarly, the ICI term in Eq. (17) can be presented by

$$Y_{IM,i} = \frac{1}{2}\sum_{\substack{L=0 \\ L\neq M}}^{N/2-1} d_{L,i}\left(-\psi_{2(M-L)+1} + \right.$$

$$\left. + 2\psi_{2(M-L)} - \psi_{2(M-L)-1}\right) = j\sum_{\substack{L=0 \\ L\neq M}}^{N/2-1} d_{L,i}\Theta_{L-M}, \quad (20)$$

where

$$\Theta_{L-M} = \frac{2}{N}\sum_{k=0}^{N-1} \sin^2\left(\frac{\pi k}{N}\right)\exp\left(\frac{j4\pi k(L-M)}{N}\right)\theta(k). \quad (21)$$

We will now investigate the case where phase noise is white Gaussian. In this case, no correlation between the samples of phase noise is assumed, and the possible difference between two consecutive samples is highest. The variance of the CPE can be calculated by

$$\mathrm{var}\left[\Theta_0\right] = \frac{4}{N^2}\sum_{k=0}^{N-1} \sin^4\left(\frac{\pi k}{N}\right) E\left[\left|\theta(k)\right|^2\right] = \frac{3\sigma_\theta^2}{2N}, \quad (22)$$

where σ_θ^2 is the variance of the phase noise, $\sigma_\theta^2 = E\left[\left|\theta(k)\right|^2\right]$. Note the summation in Eq. (22) is a constant, $\sum_{k=0}^{N-1} \sin^4(\pi k/N) = 3N/8$. The variance of the CPE is proportional to the variance of the phase noise. Thus the variance of the CPE is then given by

$$\mathrm{var}\left[Y_{CM,i}\right] = \frac{3\sigma_\theta^2\sigma_s^2}{2N} = \frac{3\sigma_\theta^2}{2N}. \quad (23)$$

Note we have used $\sigma_s^2 = 1$ for 4QAM. The variance of the angle in ICI is given by

$$\mathrm{var}\left[\Theta_{L-M}\right] = E\left[\Theta_{L-M}\Theta_{L-M}^*\right] =$$

$$= \frac{4}{N^2}\sum_{k=0}^{N-1} \sin^4\left(\frac{\pi k}{N}\right) E\left[\left|\theta(k)\right|^2\right] = \frac{3\sigma_\theta^2}{2N}. \quad (24)$$

Similarly, we can calculate the variance of the ICI from Eq. (17)

$$\mathrm{var}\left[Y_{IM,i}\right] = \left(\frac{N}{2}+1\right)\frac{3}{2N}\sigma_s^2\sigma_\theta^2 = \left(\frac{3}{4}+\frac{3}{2N}\right)\sigma_\theta^2. \quad (25)$$

The result indicates that the variance of ICI caused by phase noise has been significantly reduced in PCC-OFDM [3]. For a sufficiently large N, the value of ICI in PCC-OFDM is almost one quarter less than that in OFDM.

7. Effects of phase noise on SPI

The frequency offset estimator is derived for overlap PCC-OFDM systems without phase noise. When the phase noise is taken into account, the performance of the estimator is affected by the phase noise since the phase noise also contributes to the SPI. Figure 5 shows the SPI in the pres-

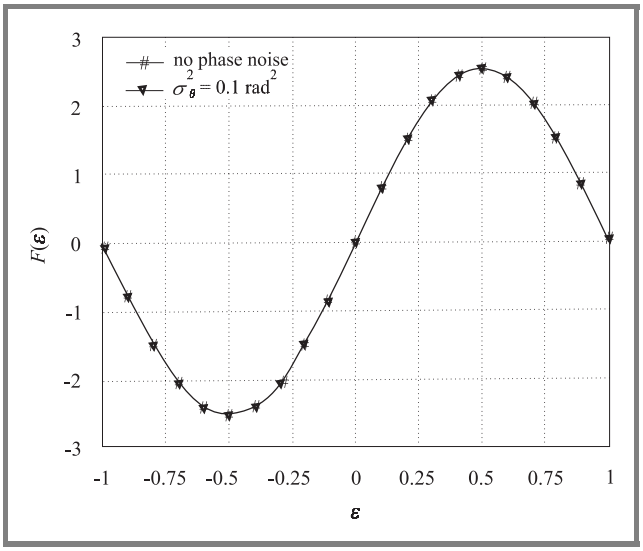

Fig. 5. Average SPI as a function of frequency offset in presence of phase noise for $N = 128$, 300 symbols.

ence of phase noise for $N = 128$ averaging over 300 symbols. It is shown that the phase noise does not significantly contribute to the SPI. In other words, the frequency offset estimator can be used for frequency offset estimation even in the presence of phase noise. Phase noise will increase the variance of estimate of frequency offset. This issue will be discussed in the next section.

8. Simulation results

To evaluate the performance of the MMSE estimator, simulations were performed. In the following simulations, 4QAM is used for the modulation scheme with $M_l = 512$ and $N = 128$. Figure 6 shows the estimator as a function of the frequency offset for $E_b/N_0 = 10$ dB. It is evident that the estimator has an approximately linear relationship with frequency offset.

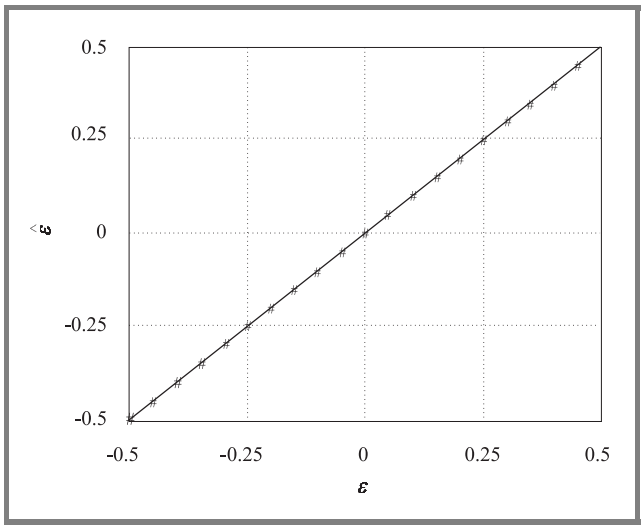

Fig. 6. $F(\varepsilon)$ as a function of frequency offset for $M_l = 512$ and $N = 128$.

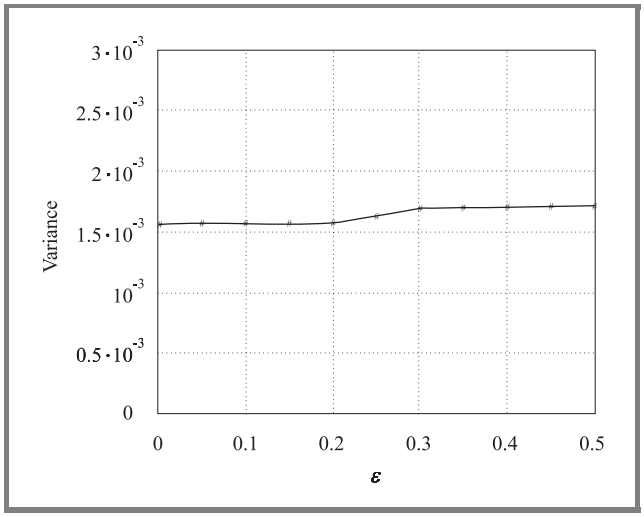

Fig. 7. Variance as a function of frequency offset for $M_l = 512$ and $N = 128$.

Figure 7 shows the variance of the frequency offset estimator as a function of the frequency offset for an ideal channel. The variance does not change significantly as frequency offset increases. This means that the overlapping components in overlap PCC-OFDM are the dominant factor for the variance. Lower variance can be obtained by increasing M_l or using a two-dimensional MMSE equalizer before the frequency offset estimation.

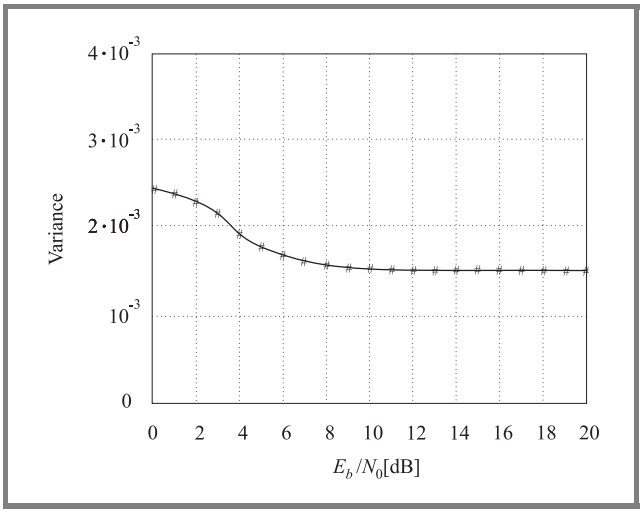

Fig. 8. Variance as a function of E_b/N_0 for $M_l = 512$ and $N = 128$.

Figure 8 shows the variance of frequency offset estimator as a function of E_b/N_0. The frequency offset simulated was zero. The variance does not significantly change as the channel noise increases. This is because the variance is dominated by the overlapping components rather than channel noise.

9. Conclusions

An MMSE frequency offset estimator for overlap PCC-OFDM systems has been presented. A frequency offset estimate is obtained by using the average SPI at the output of the receiver DFT. No training symbols or pilot tones are required. The estimator has an approximately linear relationship with frequency offset. The effects of phase noise on the performance of PCC-OFDM have been theoretically discussed. Particularly, the effect of phase noise on the SPI has been analyzed and simulated. Simulations show that the phase noise does not affect variance performance of the MMSE frequency offset estimator.

Appendix A

From Eq. (6), the power of the $2M$th subcarrier is given by

$$\begin{aligned}\left|z_{2M,i}\right|^2 = &\sum_{L=0}^{N/2-1}\left|\left(CF_{2(L-M)}+CF_{2(L-M)+1}\right)\right|^2\left|d_{L,i-1}\right|^2+\\ &+\sum_{L=0}^{N/2-1}\left|\left(CS_{2(L-M)}+CS_{2(L-M)+1}\right)\right|^2\left|d_{L,i+1}\right|^2+\\ &+\sum_{L=0}^{N/2-1}\left|\left(c_{2(L-M)}-c_{2(L-M)+1}\right)\right|^2\left|d_{L,i}\right|^2+e_{2M,i}.\end{aligned} \tag{A.1}$$

Equation (A.1) indicates that the power of each demodulated subcarrier can be represented in terms of the individual power components from the preceding, current and following PCC-OFDM symbols. Note for 4QAM with each subcarrier normalized to unity, $\left|d_{L,i}\right|^2=1$. The error term of Eq. (A.1) is then given by

$$\begin{aligned}e_{2M,i} = &\sum_{\substack{L=0\\L\neq K}}^{N/2-1}\sum_{K=0}^{N/2-1}\left(c_{2(L-M)}-c_{2(L-M)+1}\right)\left(c_{2(K-M)}-c_{2(K-M)+1}\right)^* d_{L,i}d^*_{K,i}+\\ &+\sum_{\substack{L=0\\L\neq K}}^{N/2-1}\sum_{K=0}^{N/2-1}\left(CF_{2(L-M)}+CF_{2(L-M)+1}\right)\left(CF_{2(K-M)}+CF_{2(K-M)+1}\right)^* d_{L,i-1}d^*_{K,i-1}+\\ &+\sum_{\substack{L=0\\L\neq K}}^{N/2-1}\sum_{K=0}^{N/2-1}\left(CS_{2(L-M)}+CS_{2(L-M)+1}\right)\left(CS_{2(K-M)}+CS_{2(K-M)+1}\right)^* d_{L,i+1}d^*_{K,i+1}+\\ &+\sum_{L=0}^{N/2-1}\sum_{K=0}^{N/2-1}\left(c_{2(L-M)}-c_{2(L-M)+1}\right)\left(CS_{2(K-M)}+CS_{2(K-M)+1}\right)^* d_{L,i}d^*_{K,i+1}+\\ &+\sum_{L=0}^{N/2-1}\sum_{K=0}^{N/2-1}\left(CF_{2(L-M)}+CF_{2(L-M)+1}\right)\left(c_{2(K-M)}+c_{2(K-M)+1}\right)^* d_{L,i-1}d^*_{K,i}+\\ &+\sum_{L=0}^{N/2-1}\sum_{K=0}^{N/2-1}\left(c_{2(L-M)}-c_{2(L-M)+1}\right)^*\left(CS_{2(K-M)}+CS_{2(K-M)+1}\right)d^*_{L,i}d_{K,i+1}+\\ &+\sum_{L=0}^{N/2-1}\sum_{K=0}^{N/2-1}\left(CF_{2(L-M)}+CF_{2(L-M)+1}\right)^*\left(c_{2(K-M)}+c_{2(K-M)+1}\right)d^*_{L,i-1}d_{K,i}+\\ &+2\mathrm{Re}\left\{W_{2M,i}\sum_{K=0}^{N/2-1}\left(CF_{2(K-M)}+CF_{2(K-M)+1}\right)^* d^*_{K,i-1}\right\}+\\ &+2\mathrm{Re}\left\{W_{2M,i}\sum_{K=0}^{N/2-1}\left(CS_{2(K-M)-1}+CS_{2(K-M)}\right)^* d^*_{K,i+1}\right\}+\\ &+2\mathrm{Re}\left\{W_{2M,i}\sum_{K=0}^{N/2-1}\left(c_{2(K-M)}-c_{2(K-M)+1}\right)^* d^*_{K,i}\right\}+\left|W_{2M,i}\right|^2.\end{aligned} \tag{A.2}$$

Because the expected value of all cross terms is zero, the expected value of the error term is equal to the variance of the noise. Similarly, we can obtain the power for the $(2M+1)$th subcarrier. Using $\left|d_{L,i}\right|^2 = 1$ for 4QAM, the subcarrier pair imbalance is then given by

$$\begin{aligned}
&\left|z_{2M+1,i}\right|^2 - \left|z_{2M,i}\right|^2 = \sum_{L=0}^{N/2-1} \left|\left(CF_{2(L-M)-1} + CF_{2(L-M)}\right)\right|^2 + \\
&+ \sum_{L=0}^{N/2-1} \left|\left(CS_{2(L-M)-1} + CS_{2(L-M)}\right)\right|^2 - \sum_{L=0}^{N/2-1} \left|\left(CF_{2(L-M)} + CF_{2(L-M)+1}\right)\right|^2 + \\
&- \sum_{L=0}^{N/2-1} \left|\left(CS_{2(L-M)} + CS_{2(L-M)+1'}\right)\right|^2 + \sum_{L=0}^{N/2-1} \left|\left(c_{2(L-M)-1} - c_{2(L-M)}\right)\right|^2 + \\
&- \sum_{L=0}^{N/2-1} \left|\left(c_{2(L-M)} - c_{2(L-M)+1}\right)\right|^2 + e_{2M+1,i} - e_{2M,i}\,.
\end{aligned} \tag{A.3}$$

It is shown in Appendix B that the combination of the first four summations in Eq. (A.3) equals zero. Thus we can obtain the subcarrier pair imbalance

$$F(\varepsilon) = \left|z_{2M+1,i}\right|^2 - \left|z_{2M,i}\right|^2 = S(\varepsilon) + e'_{M,i} \tag{A.4}$$

where $S(\varepsilon)$ is given by [6]

$$S(\varepsilon) = K \sin(\pi\varepsilon) \tag{A.5}$$

K is a factor defined in Eq. (11). $e'_{M,i}$ is the Mth total error, $e'_{m,i} = e_{2M+1,i} - e_{2M,i}$. In overlap PCC-OFDM, the error term is more complicated than in PCC-OFDM [8]. However, the dominant distribution in the error term is still Gaussian. As for PCC-OFDM, $e'_{M,i}$ can be approximated as AWGN with zero mean. The variance is larger than that of PCC-OFDM because of the overlapping components. Appendix C shows the variance of the coupling-crossing terms for $e'_{M,i}$. Thus, for a small frequency offset, the overall approximate variance is given by

$$e'_{M,i} \sim N(0, 8 + 8\sigma_n^2 + 2\sigma_n^4) \tag{A.6}$$

where "$\sim$" means distributed as. Note that we have used $\sigma_s^2 = 1$ for 4QAM in Eq. (A.6). The SPI estimator is therefore given by

$$\hat{\varepsilon} = \frac{1}{\pi} \sin^{-1}\left(\frac{1}{KM_l} \sum_{i=1}^{M_l} F_i(\varepsilon)\right). \tag{A.7}$$

Appendix B

The element of the first summation of Eq. (A.3) is given by

$$\begin{aligned}
&\left|\left(CF_{2(L-M)-1} + CF_{2(L-M)}\right)\right|^2 = \\
&= \frac{\sin^2\left(\frac{\pi\varepsilon}{2}\right)}{N^2 \sin^2\left(\frac{\pi(2L+\varepsilon)}{N}\right)} + \frac{\cos^2\left(\frac{\pi\varepsilon}{2}\right)}{N^2 \sin^2\left(\frac{\pi(2L-1+\varepsilon)}{N}\right)} + \\
&- \frac{\sin(\pi\varepsilon)}{N^2 \sin\left(\frac{\pi(2L+\varepsilon)}{N}\right) \sin\left(\frac{\pi(2L-1+\varepsilon)}{N}\right)} \sin\left(\frac{\pi}{N}\right).
\end{aligned} \tag{B.1}$$

The element of the second summation of Eq. (A.3) is given by

$$\left|\left(CS_{2(L-M)-1}+CS_{2(L-M)}\right)\right|^2 =$$

$$= \frac{\sin^2\left(\frac{\pi\varepsilon}{2}\right)}{N^2\sin^2\left(\frac{\pi(2L+\varepsilon)}{N}\right)} + \frac{\cos^2\left(\frac{\pi\varepsilon}{2}\right)}{N^2\sin^2\left(\frac{\pi(2L-1+\varepsilon)}{N}\right)} +$$

$$+ \frac{\sin(\pi\varepsilon)}{N^2\sin\left(\frac{\pi(2L+\varepsilon)}{N}\right)\sin\left(\frac{\pi(2L-1+\varepsilon)}{N}\right)}\sin\left(\frac{\pi}{N}\right). \tag{B.2}$$

Similarly the third and fourth terms in Eq. (A.3) can be derived.

Substituting the elements derived to the combination of the first four summations of Eq. (A.3) gives

$$\sum_{L=0}^{N/2-1}\left|\left(CF_{2(L-M)-1}+CF_{2(L-M)}\right)\right|^2+\sum_{L=0}^{N/2-1}\left|\left(CS_{2(L-M)-1}+CS_{2(L-M)}\right)\right|^2+$$

$$-\sum_{L=0}^{N/2-1}\left|\left(CF_{2(L-M)}+CF_{2(L-M)+1}\right)\right|^2-\sum_{L=0}^{N/2-1}\left|\left(CS_{2(L-M)}+CS_{2(L-M)+1}\right)\right|^2 =$$

$$= 2\sum_{L=0}^{N/2-1}\left\{\frac{\cos^2\left(\frac{\pi\varepsilon}{2}\right)}{N^2\sin^2\left(\frac{\pi(2L+\varepsilon-1)}{N}\right)}-\frac{\cos^2\left(\frac{\pi\varepsilon}{2}\right)}{N^2\sin^2\left(\frac{\pi(2L+1+\varepsilon)}{N}\right)}\right\}=0. \tag{B.3}$$

Appendix C

The coupling-cross terms $CC_{2M,i}$ in Eq. (A.2) is given by

$$CC_{2M,i} =$$

$$= \sum_{L=0}^{N/2-1}\sum_{K=0}^{N/2-1}\left(c_{2(L-M)}-c_{2(L-M)+1}\right)\left(CS_{2(K-M)}+CS_{2(K-M)+1}\right)^* d_{L,i}d^*_{K,i+1}+$$

$$+ \sum_{L=0}^{N/2-1}\sum_{K=0}^{N/2-1}\left(CF_{2(L-M)}+CF_{2(L-M)+1}\right)\left(c_{2(K-M)}-c_{2(K-M)+1}\right)^* d_{L,i-1}d^*_{K,i}+$$

$$+ \sum_{L=0}^{N/2-1}\sum_{K=0}^{N/2-1}\left(c_{2(L-M)}-c_{2(L-M)+1}\right)^*\left(CS_{2(K-M)}+CS_{2(K-M)+1}\right)d^*_{L,i}d_{K,i+1}+$$

$$+ \sum_{L=0}^{N/2-1}\sum_{K=0}^{N/2-1}\left(CF_{2(L-M)}+CF_{2(L-M)+1}\right)^*\left(c_{2(K-M)}-c_{2(K-M)+1}\right)d^*_{L,i-1}d_{K,i}. \tag{C.1}$$

Similarly, the coupling-cross terms $CC_{2M+1,i}$ for the $(2M+1)$th error term can also be obtained. Note the first term and the third term are mutually conjugated, the second term and the fourth term are mutually conjugated in Eq. (C.1). Thus, $CC_{2M+1,i} - CC_{2M,i}$ can be written as

$$CC_{2M+1,i} - CC_{2M,i} =$$

$$= -2\mathrm{Re}\left\{ d_{M,i} \sum_{K=0}^{N/2-1} \left(CS_{2(K-M)-1} + 2CS_{2(K-M)} + CS_{2(K-M)+1} \right)^* d^*_{K,i+1} \right\} +$$

$$- 2\mathrm{Re}\left\{ d^*_{M,i} \sum_{L=0}^{N/2-1} \left(CF_{2(L-M)-1} + 2CF_{2(L-M)} + CF_{2(L-M)+1} \right) d_{L,i-1} \right\}, \tag{C.2}$$

where $\mathrm{Re}(\bullet)$ represents the real part of a complex number. For the first summation in Eq. (C.2), considering the most significant complex coefficients CS_0, we get

$$d_{M,i} \sum_{K=0}^{N/2-1} \left(CS_{2(K-M)-1} + 2CS_{2(K-M)} + CS_{2(K-M)+1} \right)^* d^*_{K,i+1} \approx$$

$$\approx 2 d_{M,i} CS_0^* d^*_{M,i+1} \,. \tag{C.3}$$

Similarly, we can also simplify the second summation in Eq. (C.2). In addition, in the absence of frequency offset, the value of the most significant complex coefficient can be obtained from Eqs. (7) and (8), that is $CS_0 = CF_0 = 0.5$. Thus Eq. (C.2) can be written as

$$CC_{2M+1,i} - CC_{2M,i} \approx$$

$$\approx -2\mathrm{Re}\left\{ d_{M,i} d^*_{M,i+1} \right\} - 2\mathrm{Re}\left\{ d^*_{M,i} d_{M,i-1} \right\}. \tag{C.4}$$

The variance of the left side of Eq. (C.4) is given by

$$E\left[\left| CC_{2M+1,i} - CC_{2M,i} \right| \right]^2 \approx$$

$$\approx E\left[4\left(\mathrm{Re}\left(d_{M,i} d^*_{M,i+1} \right) \right)^2 + 4\left(\mathrm{Re}\left(d^*_{M,i} d_{M,i-1} \right) \right)^2 + \right.$$

$$\left. + 4\left(\mathrm{Re}\left(d_{M,i} d^*_{M,i+1} \right) \right) \left(\mathrm{Re}\left(d^*_{M,i} d_{M,i-1} \right) \right) \right] = 8\sigma_s^4 \,. \tag{C.5}$$

When all complex coefficients are considered, the variance will be slightly larger than above result. Please note that this result is obtained under the assumption of no frequency offset. In the presence of a small frequency offset, the variance could be slightly larger.

References

[1] ETSI, ETS 300 744, "Digital video broadcasting: frame structure, channel coding and modulation for digital terrestrial television", Aug. 1997.

[2] ETSI, DTS/BRAN 0023003, V0.k., "Broadband radio access networks; HiperLAN type 2 technical specification; Physical layer", Aug. 1999.

[3] J. Stott, "The effects of phase noise in COFDM", BBC Research and Development EBU Technical Review, 1998.

[4] J. Armstrong, "Analysis of new and existing methods of reducing intercarrier interference due to carrier frequency offset in OFDM", *IEEE Trans. Commun.*, vol. 47, no. 3, pp. 365–369, 1999.

[5] Y. Zhao and S. G. Haggman, "Sensivity to Doppler shift and carrier frequency errors in OFDM systems – the consequences and solutions", in *IEEE 46th Veh. Technol. Conf.*, Atlanta, USA, Apr. 1996, vol. 3, pp. 1564–1568.

[6] J. Armstrong, P. M. Grant, and G. Povey, "Polynomial cancellation coding of OFDM to reduce intercarrier interference due to Doppler spread", in *IEEE Globecom*, Nov. 1998, vol. 5, pp. 2771–2776.

[7] J. Shentu and J. Armstrong, "Effects of phase noise on the performance of PCC-OFDM", in *Proc. WITSP'2002*, Australia, Dec. 2002, pp. 50–54.

[8] J. Shentu, J. Armstrong, and G. Tobin, "MMSE frequency offset estimator for PCC-OFDM", in *IEEE MICC'2001*, Kuala Lumpur, Oct. 2001, pp. 304–309.

[9] J. Armstrong, J. Shentu, and C. Tellambura, "Frequency domain equalization for OFDM systems with mapping data onto subcarrier pairs and overlapping symbol periods", in *Proc. 5th Int. Symp. Commun. Theory & Appl.*, UK, July 1999, pp. 102–104.

[10] J. Shentu and J. Armstrong, "Frequency offset estimation for PCC-OFDM with symbols overlapped in the time domain", in *Proc. WITSP'2002*, Australia, Dec. 2002, pp. 72–79.

[11] J. Shentu and J. Armstrong, "Blind frequency offset estimation for PCC-OFDM with symbols overlapped in the time domain", in *Proc. IEEE ISCAS'2001*, Sydney, May 2001, vol. 4, pp. 570–573.

[12] J. Shentu and J. Armstrong, "A new frequency offset estimator for OFDM", in *Commun. Syst. Netw. Digit. Signal Proc.*, A. C. Boucouvalas, Ed., UK, July 2000, pp. 13–16.

[13] A. Papoulis, *Probability, Random Variables and Stochastic Processes*. McGraw-Hill, 1981.

[14] A. Ronald Gallant, *Nonlinear Statistical Models*. Wiley, 1987.

[15] J. Shentu, K. Panta, and J. Armstrong, "Effects of phase noise on the performance of OFDM systems using an ICI cancellations scheme" (accepted for publication by *IEEE Trans. Broadcast.*, 2003).

[16] A. G. Armada, "Phase noise and sub-carrier spacing effects on the performance of an OFDM communication systems", *IEEE Commun. Lett.*, vol. 2, no. 1, 1998.

[17] A. R. S. Bahai and B. R. Saltzberg, *Multicarrier Digital Communications: Theory and Applications of OFDM*. New York: Kluwer, 1999.

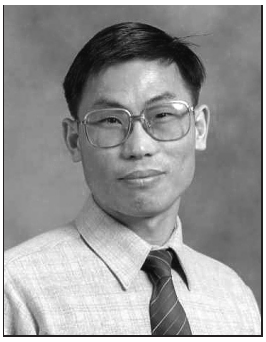

Jinwen Shentu received a B.Eng. and an M.Eng. from Lanzhou Jiaotong University (former Lanzhou Railway University), China in 1984 and 1991 respectively, and a Ph.D. from La Trobe University, Melbourne, Australia in 2001. From 1984 to 1988, he was a teacher at Neijiang Railway Mechanical School, Sichuan, China. From 1991 to 1997 he worked as an electronic engineer/senior engineer in Shanghai Railway Communication Equipment Factory, Shanghai, China. He is currently working as a research staff at the Department of Electronic Engineering, La Trobe University. His research interests include OFDM, synchronization, channel estimation, broadband wireless networking and signal processing.
e-mail: j.shentu@ee.latrobe.edu.au
Department of Electronic Engineering
La Trobe University
Victoria 3086, Australia

Jean Armstrong received a B.Sc. in electrical engineering from the University of Edinburgh, Scotland in 1974, an M.Sc. in digital techniques from Heriot-Watt University, Edinburgh, Scotland in 1980 and a Ph.D. in digital communications from Monash University, Melbourne, Australia in 1993. From 1974–1977 she worked as a design engineer at Hewlett-Packard Ltd., Scotland. In 1977 she was appointed as a Lecturer in electrical engineering at the University of Melbourne, Australia. Since 1977 she has held a variety of academic positions at the University of Melbourne, Monash University and La Trobe University. Her research interests include digital communications, engineering education and women in engineering and she has published over 50 research papers. She is currently an Associate Professor at La Trobe University.
e-mail: j.armstrong@latrobe.edu.au
Department of Electronic Engineering
La Trobe University
Victoria 3086, Australia